ACHIEVABLE MSE/SNR/BEP/RATE REGIONS FOR DECENTRALIZED RECEIVERS

Raphael Hunger, Michael Joham, and Wolfgang Utschick

9th International ITG/IEEE Workshop on Smart Antennas (WSA 2005)
Duisburg, Germany
April 4th–5th, 2005

Munich University of Technology
Institute for Circuit Theory and Signal Processing
http://www.nws.ei.tum.de

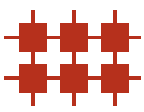

ACHIEVABLE MSE/SNR/BEP/RATE REGIONS FOR DECENTRALIZED RECEIVERS

Raphael Hunger, Michael Joham, and Wolfgang Utschick

Institute for Circuit Theory and Signal Processing
Munich University of Technology
80290 Munich, Germany
E-Mail: {Hunger, Joham, Utschick}@nws.ei.tum.de

ABSTRACT

We present a modified precoding scheme for the downlink of a multi-user broadcast scenario facilitating the simple assignment of arbitrary *mean square errors*, *signal-to-noise ratios*, *bit error probabilities*, or *data rates*. Based on a constrained zero-forcing filter at the transmitter side with power loading for the individual users, a complete set of achievable regions can easily be reported to higher OSI layers, which then feature the possibility to choose a desired element of these regions according to some given quality of service request for example. For our linear precoding filter, all regions turn out to be convex, whereas non-convex regions are obtained when the non-linear Tomlinson-Harashima precoding (THP) is applied in combination with the zero-forcing feedforward filter.

1. INTRODUCTION

In the downlink of a time-division duplex system, the channel coefficients describing the transmission from the base-station to the receivers are available at the transmitter side due to the reciprocity of the channel. Hence, multi-user interference can be combated by a precoding scheme performing the channel equalization *before* the transmission over the channel takes place. This kind of transmit processing can for example be found in [1, 2, 3, 4, 5, 6, 7], or [8]. In contrast to the general MIMO system with *fully cooperative* receivers (e.g. [9, 10]), where channel equalization can be performed by *both* transmitter and receiver, the transmitter has to suppress the multi-user interference alone when the receivers are non-cooperative or decentralized. A commonly used cost function underlying the optimization of many precoders for such a scenario is the *sum* mean square error, since the appropriate transmit filter can be computed analytically, cf. [1, 11]. The arising *mean square errors* (MSEs) of the *individual* users depend on the channel realization and can hardly be described.

Our new approach directly relates the MSEs of the users to each other instead of focusing on the sum MSE alone. By means of a zero-forcing filter at the transmitter with power loading for the receivers, we decouple the channel into parallel AWGN channels allowing for a convenient assignment of *mean square errors* (MSEs), *signal-to-noise ratios* (SNRs), *bit error probabilities* (BEPs), or *data rates* (DRs) to the individual users. Given a maximum transmit power and the parameters describing the transmission over the wireless channel, the physical layer of the OSI system reports the supported MSE, SNR, BEP, and DR regions to the higher layers. Then, the upper layers decide, which operating point fits best to the quality of service requested by the users.

2. SYSTEM MODEL AND NOTATION

The downlink of the broadcast channel is depicted in Fig. 1. Data symbols $s_k \in \mathbb{C}$ of the K users are stacked in

$$\boldsymbol{s} = [s_1, \ldots, s_K]^{\mathrm{T}} \in \mathbb{C}^K,$$

whose correlation matrix $\boldsymbol{R_s} = \mathrm{E}[\boldsymbol{s}\boldsymbol{s}^{\mathrm{H}}] = \mathbf{diag}\{\sigma_{s_k}^2\}_{k=1}^K$ is assumed to be diagonal, i.e., the symbols of the users are uncorrelated. The precoding matrix

$$\boldsymbol{P} = [\boldsymbol{p}_1, \ldots, \boldsymbol{p}_K] \in \mathbb{C}^{N_{\mathrm{a}} \times K}$$

transforms the K data symbols into the baseband signal $\boldsymbol{y} = \boldsymbol{P}\boldsymbol{s} \in \mathbb{C}^{N_{\mathrm{a}}}$. Assuming a frequency flat channel, the transmission from the N_{a} transmitting antennas to the K receivers, each having a single antenna element, is described by the channel matrix

$$\boldsymbol{H} = [\boldsymbol{h}_1, \ldots, \boldsymbol{h}_k]^{\mathrm{T}} \in \mathbb{C}^{K \times N_{\mathrm{a}}}.$$

We assume $\boldsymbol{H}$ to be perfectly known, otherwise robust paradigms have to be applied, cf. [12, 13]. At the receiver side, noise contributions

$$\boldsymbol{\eta} = [\eta_1, \ldots, \eta_K]^{\mathrm{T}} \in \mathbb{C}^K$$

are added, and finally, positive scalar weights $b_k \in \mathbb{R}_+$ recover the amplitude due to the path loss. In contrast to the

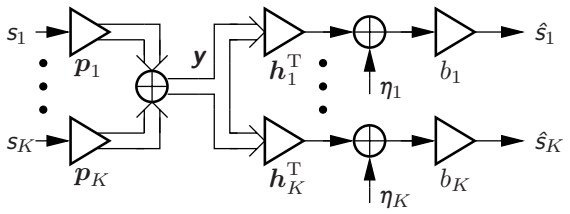

Figure 1. Downlink of the multi-user broadcast scenario.

commonly used assumption that all users have to apply the same weight $b_k = b$ as automatic gain control, we allow different weights b_k yielding a modified filter structure at the transmitter side, compare with [5, 7]. In matrix vector notation, we have

$$\hat{\boldsymbol{s}} = \boldsymbol{BHP}\boldsymbol{s} + \boldsymbol{B}\boldsymbol{\eta} \in \mathbb{C}^K, \tag{1}$$

where we introduced the diagonal matrix

$$\boldsymbol{B} = \mathbf{diag}\{b_1, \ldots, b_K\} \in \mathbb{R}_+^{K\times K} \tag{2}$$

comprising the elements $b_k\ \forall k$. Note that the diagonal structure of $\boldsymbol{B}$ reflects the decentralized scenario, since the users cannot cooperate.

Notation: Deterministic vectors and matrices are denoted by lower and upper case bold letters, whereas the respective random variables are written in sans serif font. The operators $\mathrm{E}[\cdot]$, $(\cdot)^{\mathrm{T}}$, and $(\cdot)^{\mathrm{H}}$ stand for expectation with respect to symbols and noise, transposition, and Hermitian transposition, respectively. $\boldsymbol{I}_K$ stands for the $K \times K$ identity matrix whose kth column is $\boldsymbol{e}_k$, and $\mathbf{diag}\{\cdot\}$ generates a diagonal matrix whose elements are the argument of the **diag** operator. The entry in row a and column b of a Matrix $\boldsymbol{A}$ is denoted by $[\boldsymbol{A}]_{a,b}$.

3. REGIONS SUPPORTED BY THE LINEAR CONSTRAINED ZERO-FORCING FILTER

The kernel of our new approach is a constrained zero-forcing filter at the transmitter side allowing for a power loading of the individual users. Therefore, we require the precoder to decouple the interference afflicted streams into parallel AWGN channels, see Fig. 2. The resulting MSEs

$$\varepsilon_k = \mathrm{E}[|\hat{\mathsf{s}}_k - \mathsf{s}_k|^2] \tag{3}$$

are minimized in sum *constrained on* a given MSE ratio

$$a_k = \frac{\varepsilon_1}{\varepsilon_k}, \quad a_1 = 1. \tag{4}$$

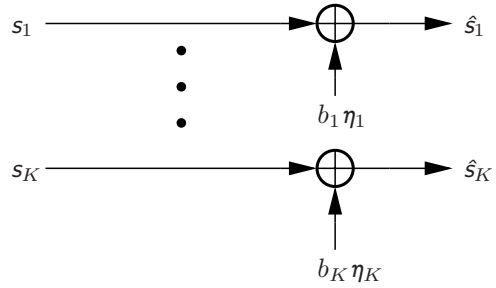

Figure 2. Overall transfer function of the constrained zero-forcing filter resulting in parallel AWGN channels with different (weighted) noise contributions.

The linear transmit filter $\boldsymbol{P}_{\mathrm{CZF}}$ and the user weights $b_{\mathrm{CZF},k}$, $k \in \{1, \ldots, K\}$, follow from the optimization

$$\begin{aligned}\{\boldsymbol{P}_{\mathrm{CZF}}, b_{\mathrm{CZF},1}, \ldots, b_{\mathrm{CZF},K}\} = &\underset{\{\boldsymbol{P}, b_1, \ldots, b_K\}}{\operatorname{argmin}} \sum_{k=1}^{K} \varepsilon_k \\ \text{subject to: } &\boldsymbol{BHP} = \boldsymbol{I}_K, \\ &\mathrm{E}[\|\boldsymbol{P}\boldsymbol{s}\|_2^2] \le E_{\mathrm{tr}}, \\ &\varepsilon_1 = a_k \varepsilon_k \ \ \forall k.\end{aligned} \tag{5}$$

The first constraint in (5) completely removes the multi-user interference and ensures unbiasedness, whereas the second one limits the symbol-averaged dissipated energy. Finally, certain MSE quotients $a_2, \ldots, a_K$ must be achieved. Due to $\boldsymbol{BHP} = \boldsymbol{1}_K$, the single-user mean squared errors reduce to

$$\varepsilon_k = b_k^2 \sigma_{\eta_k}^2, \tag{6}$$

with the average noise power $\sigma_{\eta_k}^2 = \mathrm{E}[|\eta_k|^2]$. Solving (5) leads to the precoding matrix

$$\begin{aligned}\boldsymbol{P}_{\mathrm{CZF}} &= \boldsymbol{H}^{\mathrm{H}}(\boldsymbol{H}\boldsymbol{H}^{\mathrm{H}})^{-1}\boldsymbol{B}_{\mathrm{CZF}}^{-1} \\ &= \boldsymbol{H}^{\mathrm{H}}(\boldsymbol{H}\boldsymbol{H}^{\mathrm{H}})^{-1}\mathbf{diag}\{b_{\mathrm{CZF},k}^{-1}\}_{k=1}^{K},\end{aligned} \tag{7}$$

achieving the single-user MSEs

$$\varepsilon_k = \frac{1}{E_{\mathrm{tr}} a_k} \sum_{m=1}^{K} a_m \sigma_{\mathsf{s}_m}^2 \sigma_{\eta_m}^2 \left[\left(\boldsymbol{H}\boldsymbol{H}^{\mathrm{H}}\right)^{-1}\right]_{m,m}. \tag{8}$$

Note that the user weights $b_{\mathrm{CZF},k}$ follow from (6) and (8). For the $K = 2$ users scenario, (8) boils down to

$$\begin{aligned}\varepsilon_1 &= \frac{1}{E_{\mathrm{tr}}(1-|\varrho|^2)}\left(\frac{\sigma_{\mathsf{s}_1}^2\sigma_{\eta_1}^2}{\|\boldsymbol{h}_1\|_2^2} + a_2\frac{\sigma_{\mathsf{s}_2}^2\sigma_{\eta_2}^2}{\|\boldsymbol{h}_2\|_2^2}\right) \\ \varepsilon_2 &= \frac{1}{E_{\mathrm{tr}}(1-|\varrho|^2)}\left(\frac{\sigma_{\mathsf{s}_1}^2\sigma_{\eta_1}^2}{a_2\|\boldsymbol{h}_1\|_2^2} + \frac{\sigma_{\mathsf{s}_2}^2\sigma_{\eta_2}^2}{\|\boldsymbol{h}_2\|_2^2}\right),\end{aligned} \tag{9}$$

with the 'orthogonality' factor

$$\varrho = \frac{\boldsymbol{h}_1^{\mathrm{T}}\boldsymbol{h}_2^*}{\|\boldsymbol{h}_1\|_2\|\boldsymbol{h}_2\|_2} \tag{10}$$

describing the colinearity between the channels $\boldsymbol{h}_1$ and $\boldsymbol{h}_2$ of the two users. Obviously, when $\boldsymbol{h}_1$ is a scaled version of $\boldsymbol{h}_2$, the magnitude of the orthogonality factor is $|\varrho| = 1$, and the two MSEs ε_1 and ε_2 go to infinity, since the mutual interference cannot be suppressed by the zero-forcing filter.

3.1. Mean Square Error (MSE) Regions

When eliminating the MSE quotients a_k ($k \in \{2, \ldots, K\}$) in (8), an implicit description of the possible MSE values reads as

$$E_{\mathrm{tr}} = \sum_{k=1}^{K} \frac{\sigma_{s_k}^2 \sigma_{\eta_k}^2 \left[\left(\boldsymbol{H}\boldsymbol{H}^{\mathrm{H}} \right)^{-1} \right]_{k,k}}{\varepsilon_k}. \tag{11}$$

allowing for the computation of the required transmit power E_{tr} given the MSE requests ε_k and the channel conditions. For $K = 2$ users, we find an explicit expression for the MSE ε_2 of user 2 depending on the MSE ε_1 of user 1:

$$\varepsilon_2(\varepsilon_1) = \frac{\varepsilon_{\mathrm{inf},1}\varepsilon_{\mathrm{inf},2}}{\varepsilon_1 - \varepsilon_{\mathrm{inf},1}} + \varepsilon_{\mathrm{inf},2}, \tag{12}$$

with an infimum for the MSE of user k ($k \in \{1, 2\}$) reading as

$$\varepsilon_{\mathrm{inf},k} = \frac{\sigma_{s_k}^2 \sigma_{\eta_k}^2}{E_{\mathrm{tr}} \|\boldsymbol{h}_k\|_2^2} \frac{1}{1 - |\varrho|^2}, \tag{13}$$

being asymptotically achieved, when the MSE of the *other* user goes to infinity by letting $b_{3-k} \to \infty$ ($k \in \{1, 2\}$). Eq. (12) represents a shifted and weighted hyperbola, whose shifts depend on the available transmit power E_{tr} and on the instantaneous channel realization, cf. Fig. 3. The minimum *sum* MSE $\varepsilon_{\Sigma\text{-min},1} + \varepsilon_{\Sigma\text{-min},2}$ for example follows from setting $\frac{\partial}{\partial \varepsilon_1}[\varepsilon_1 + \varepsilon_2(\varepsilon_1)] = 0$ and yields

$$\begin{aligned} \varepsilon_{\Sigma\text{-min},1} &= \sqrt{\varepsilon_{\mathrm{inf},1}\varepsilon_{\mathrm{inf},2}} + \varepsilon_{\mathrm{inf},1}, \\ \varepsilon_{\Sigma\text{-min},2} &= \sqrt{\varepsilon_{\mathrm{inf},1}\varepsilon_{\mathrm{inf},2}} + \varepsilon_{\mathrm{inf},2}, \\ a_2 &= \sqrt{\frac{\varepsilon_{\mathrm{inf},1}}{\varepsilon_{\mathrm{inf},2}}} = \frac{\|\boldsymbol{h}_2\|_2}{\|\boldsymbol{h}_1\|_2} \sqrt{\frac{\sigma_{s_1}^2 \sigma_{\eta_1}^2}{\sigma_{s_2}^2 \sigma_{\eta_2}^2}}. \end{aligned} \tag{14}$$

Given a *maximum* dissipated power E_{tr}, any MSE pair $(\varepsilon_1, \varepsilon_2)$ from the convex set

$$\mathbb{S}_\varepsilon = \left\{ (\varepsilon_1, \varepsilon_2) | \varepsilon_2 \geq \frac{\varepsilon_{\mathrm{inf},1}\varepsilon_{\mathrm{inf},2}}{\varepsilon_1 - \varepsilon_{\mathrm{inf},1}} + \varepsilon_{\mathrm{inf},2} \wedge \varepsilon_1 > \varepsilon_{\mathrm{inf},1} \right\}$$

can be achieved. The second inequality is strict, since equality could only hold asymptotically by setting b_2 to infinity which corresponds to discarding the respective data stream (cf. Eq. 7 with $\boldsymbol{s}$ being left-hand multiplied by $\boldsymbol{P}_{\mathrm{CZF}}$). But then, the gain 1 constraint in $\boldsymbol{B}\boldsymbol{H}\boldsymbol{P} = \boldsymbol{I}_K$ cannot be maintained.

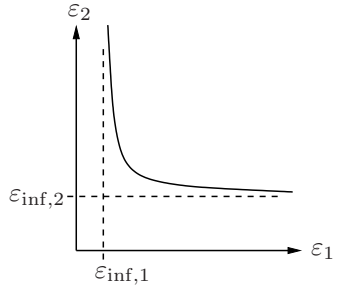

Figure 3. Shifted hyperbola describing the dependency of the user 2 MSE ε_2 on the user 1 MSE ε_1 for a *fixed* transmit power E_{tr}. Different abscissa offsets $\varepsilon_{\mathrm{inf},1}$ and ordinate offsets $\varepsilon_{\mathrm{inf},2}$ result from different instantaneous channel powers.

3.2. Signal-to-Noise Ratio (SNR) Regions

Since the transmission is decoupled into parallel AWGN channels with weighted noise variances $\varepsilon_k = b_k^2 \sigma_{\eta_k}^2$, the resulting signal-to-noise ratios read as

$$\gamma_k = \frac{\sigma_{s_k}^2}{\varepsilon_k} \in \mathbb{R}_+, \; k \in \{1, \ldots, K\}. \tag{15}$$

Introducing the substitutes for the suprema $\gamma_{\mathrm{sup},k} = \sigma_{s_k}^2 / \varepsilon_{\mathrm{inf},k}$ of the signal-to-noise ratios, (11) can be transformed into

$$\sum_{k=1}^{K} \gamma_k \sigma_{\eta_k}^2 \left[(\boldsymbol{H}\boldsymbol{H}^{\mathrm{H}})^{-1} \right]_{k,k} = E_{\mathrm{tr}}, \tag{16}$$

describing a K-dimensional hyperplane, or for the two users case (cf. Eq. 12),

$$\gamma_2(\gamma_1) = \gamma_{\mathrm{sup},2} - \gamma_1 \frac{\gamma_{\mathrm{sup},2}}{\gamma_{\mathrm{sup},1}}, \tag{17}$$

see Fig. 4 Herewith, any SNR pair (γ_1, γ_2) being element of the convex set

$$\mathbb{S}_\gamma = \left\{ (\gamma_1, \gamma_2) | 0 < \gamma_2 \leq \gamma_{\mathrm{sup},2} - \gamma_1 \frac{\gamma_{\mathrm{sup},2}}{\gamma_{\mathrm{sup},1}} \wedge 0 < \gamma_1 < \gamma_{\mathrm{sup},1} \right\}$$

is feasible for our zero-forcing approach. Note that the supremum of the *sum* SNR is $\max\{\gamma_{\mathrm{sup},1}, \gamma_{\mathrm{sup},2}\}$.

3.3. Bit Error Probability (BEP) Regions

For a QPSK modulation alphabet, the bit error probability p_k of user k is related to the mean square error ε_k and the the signal-to-noise ratio γ_k via

$$p_k = \frac{1}{2}\mathrm{erfc}\left(\frac{\sigma_{s_k}}{\sqrt{2\varepsilon_k}} \right) = \frac{1}{2}\mathrm{erfc}\left(\sqrt{\frac{\gamma_k}{2}} \right), \tag{18}$$

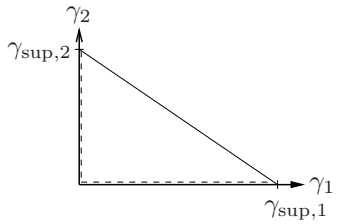

Figure 4. Dependency of the user 2 SNR γ_2 on the user 1 SNR γ_1 for a *fixed* transmit power E_{tr}.

with $\mathrm{erfc}(\cdot)$ denoting the complementary error function. Consequently, the infima of the bit error probabilities are

$$p_{\mathrm{inf},k} = \frac{1}{2}\mathrm{erfc}\left(\frac{\sigma_{\boldsymbol{s}_k}}{\sqrt{2\varepsilon_{\mathrm{inf},k}}}\right) = \frac{1}{2}\mathrm{erfc}\left(\sqrt{\frac{\gamma_{\mathrm{sup},k}}{2}}\right). \quad (19)$$

Plugging this into (12) and (17), respectively, we obtain for the $K = 2$ users case

$$\begin{aligned} p_2(p_1) &= \frac{1}{2}\mathrm{erfc}\left(\sqrt{\frac{\sigma_{\boldsymbol{s}_2}^2}{2\varepsilon_{\mathrm{inf},2}} - \frac{\sigma_{\boldsymbol{s}_2}^2\varepsilon_{\mathrm{inf},1}}{\sigma_{\boldsymbol{s}_1}^2\varepsilon_{\mathrm{inf},2}}\mathrm{erfcinv}^2(2p_1)}\right) \\ &= \frac{1}{2}\mathrm{erfc}\left(\sqrt{\frac{\gamma_{\mathrm{sup},2}}{2} - \frac{\gamma_{\mathrm{sup},2}}{\gamma_{\mathrm{sup},1}}\mathrm{erfcinv}^2(2p_1)}\right). \end{aligned} \quad (20)$$

Here, $\mathrm{erfcinv}(\cdot)$ denotes the inverse of the complementary error function $\mathrm{erfc}(\cdot)$. Any bit error probability pair (p_1, p_2) can be reached that lies in the convex set

$$\mathbb{S}_p = \{(p_1,p_2) | 0.5 > p_2 \geq p_2(p_1) \wedge 0.5 > p_1 > p_{\mathrm{inf},1}\}.$$

3.4. Data Rate (DR) Regions

Mapping the signal-to-noise ratios to (normalized) data rates follows from the relationship

$$R_k = \log_2(1+\gamma_k), \quad (21)$$

with the suprema of the data rates

$$R_{\mathrm{sup},k} = \log_2(1+\gamma_{\mathrm{sup},k}), \quad (22)$$

which are asymptotically achieved when the data rate of the (other) user $3-k$ goes down to zero by setting $b_{3-k} \to \infty$ but maintaining the orthogonality constraint $\boldsymbol{h}_{3-k}^{\mathrm{T}}\boldsymbol{p}_k = 0$. Whether the users apply their scalar weights b_k or not does not influence the possible data rate, since both desired signal and noise are scaled by the same factor without a change of the signal-to-noise ratio. The data rate R_2 of user 2 depending on the data rate R_1 of user 1 thus reads as

$$R_2(R_1) = \log_2\left(1 + \frac{2^{R_{\mathrm{sup},2}}-1}{2^{R_{\mathrm{sup},1}}-1}(2^{R_{\mathrm{sup},1}} - 2^{R_1})\right). \quad (23)$$

When we maximize the sum rate $R_1 + R_2$, two cases occur:

3.4.1. The following two inequalities hold

$$2^{R_{\mathrm{sup},1}+1} \leq 2^{R_{\mathrm{sup},1}+R_{\mathrm{sup},2}} + 1, \quad (24)$$
$$2^{R_{\mathrm{sup},2}+1} \leq 2^{R_{\mathrm{sup},1}+R_{\mathrm{sup},2}} + 1. \quad (25)$$

Then, the rates $R_{\Sigma-\max,k}$ achieving maximum sum rate are

$$R_{\Sigma-\max,k} = \log_2\left(\frac{2^{R_{\mathrm{sup},1}+R_{\mathrm{sup},2}}-1}{2^{R_{\mathrm{sup},3-k}}-1}\right) - 1. \quad (26)$$

The difference $R_{\Sigma-\max,1} - R_{\Sigma-\max,2}$ only depends on the ratio of the channel and noise powers, i.e.

$$R_{\Sigma-\max,1} - R_{\Sigma-\max,2} = \log_2\left(\frac{\sigma_{\eta_2}^2\|\boldsymbol{h}_1\|_2^2}{\sigma_{\eta_1}^2\|\boldsymbol{h}_2\|_2^2}\right). \quad (27)$$

3.4.2. Either (24) or (25) does not hold

When $R_{\mathrm{sup},1} \geq R_{\mathrm{sup},2}$, the sum data rate is maximized by discarding user 2:

$$R_{\Sigma-\max,1} \to R_{\mathrm{sup},1} \text{ and } R_{\Sigma-\max,2} \to 0. \quad (28)$$

When $R_{\mathrm{sup},1} < R_{\mathrm{sup},2}$, indices have to be interchanged:

$$R_{\Sigma-\max,2} \to R_{\mathrm{sup},2} \text{ and } R_{\Sigma-\max,1} \to 0. \quad (29)$$

If (28) has to be applied, the constraint $\boldsymbol{h}_2^{\mathrm{T}}\boldsymbol{p}_1 = 0$ in (5) could be dropped to further increase the data rate, since then, the 'orthogonality' factor ϱ in (9) diminishes and for the MSE quotient a_2, we find $a_2 \to 0$. The same holds, if (29) has to be applied, only indices have to be interchanged, and $a_2 \to \infty$.
Summing up, the data rates achieving maximum sum rate lie on piecewise affine straight lines.

4. REGIONS SUPPORTED BY THE CONSTRAINED ZERO-FORCING FILTER WITH NON-LINEAR TOMLINSON-HARASHIMA PRECODING

The framework presented in the previous chapter can be transferred to a non-linear scheme with Tomlinson-Harashima precoding [11], [14], [15], [16], and [17]. To this end, we extend the system from Fig. 1 by adding non-linear *modulo* operations $\mathbf{M}(\cdot)$ at both transmitter (cf. Fig 5) and receivers. At the transmitter side, this *modulo* operation keeps both real and imaginary parts of each entry in $\boldsymbol{v}$ upper bounded in magnitude. Moreover, a spatial feedback filter $\boldsymbol{F}$ which has to be lower triangular with zeros on the main diagonal (due to realizability) feeds back the already precoded symbols in $\boldsymbol{v}$. A unitary permutation matrix

$$\boldsymbol{\Pi} = \sum_{k=1}^{K} \boldsymbol{e}_k \boldsymbol{e}_{i_k}^{\mathrm{T}} \in \{0,1\}^{K\times K} \quad (30)$$

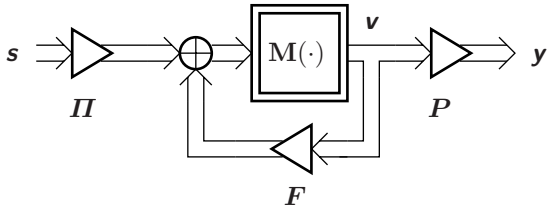

Figure 5. Transmitter extended by a *modulo* operation $\mathbf{M}(\cdot)$ and a spatial feedback filter $\boldsymbol{F}$.

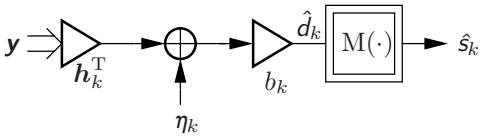

Figure 6. Single receiver branch for user k when THP is applied.

allows for different sorting orders from which additional gains can be achieved. The index i_k denotes the user who is precoded at the kth step. A quasi-linear representation of the *modulo* operation is obtained by shifting $\mathbf{M}(\cdot)$ out of the feedback loop and replacing it by an auxiliary summand $\boldsymbol{\Pi}^{\mathrm{T}}\boldsymbol{a}$, which then shall be revoked by the modulo operations at the receivers, see Fig. 7. Now, all filter computations rest upon the vector

$$\boldsymbol{d} = \boldsymbol{\Pi}^{\mathrm{T}}(\boldsymbol{I}_K - \boldsymbol{F})\boldsymbol{v} \in \mathbb{C}^K. \tag{31}$$

The correlation matrix $\boldsymbol{R}_{\boldsymbol{v}}$ of $\boldsymbol{v}$ is diagonal with

$$\boldsymbol{R}_{\boldsymbol{v}} = \mathrm{E}[\boldsymbol{v}\boldsymbol{v}^{\mathrm{H}}] = \mathbf{diag}\{\sigma_{v_k}^2\}_{k=1}^K \in \mathbb{R}_+^{K\times K}, \tag{32}$$

since symbols that ran through the modulo device are assumed to be uncorrelated among each other. Under the assumption, that the symbol correlation matrix is a scaled identity matrix, i.e., $\boldsymbol{R}_{\boldsymbol{s}} = \sigma_{\boldsymbol{s}}^2\boldsymbol{I}_K$, the entries of $\boldsymbol{R}_{\boldsymbol{v}}$ are $\sigma_{v_1}^2 = \sigma_{\boldsymbol{s}}^2$ and $\sigma_{v_k}^2 = \frac{M}{M-1}\sigma_{\boldsymbol{s}}^2\ \forall k \in \{2,\ldots,K\}$ for an M-ary QAM modulation alphabet with $M = 4^m$, $m \in \mathbb{N}$, see [15] for example. The interference removal constraint in (5) slightly changes due to the THP and reads as

$$\boldsymbol{B}\boldsymbol{H}\boldsymbol{P} = \boldsymbol{\Pi}^{\mathrm{T}}(\boldsymbol{I}_K - \boldsymbol{F}), \tag{33}$$

and the individual MSEs are (see Fig. 6)

$$\begin{aligned}\varepsilon_k &= \mathrm{E}[|[\boldsymbol{d}]_{k,k} - \hat{d}_k|^2] \\ &= \mathrm{E}[|[\boldsymbol{d}]_{k,k} - b_k\boldsymbol{h}_k^{\mathrm{T}}\boldsymbol{P}\boldsymbol{v} - b_k\eta_k|^2] \in \mathbb{R}_+,\end{aligned} \tag{34}$$

which reduce due to (33) to

$$\varepsilon_k = b_k^2\sigma_{\boldsymbol{\eta}_k}^2, \tag{35}$$

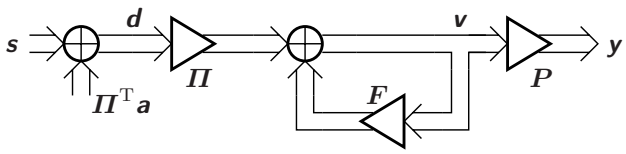

Figure 7. Quasi-linear representation of the THP without modulo operation $\mathbf{M}(\cdot)$ but auxiliary signal $\boldsymbol{\Pi}^{\mathrm{T}}\boldsymbol{a}$ instead.

so we have the same expression as in (6) for the linear filter. The optimization from (5) now reads as

$$\begin{aligned}\{\boldsymbol{P}_{\mathrm{CZF}}, \boldsymbol{B}_{\mathrm{CZF}}, \boldsymbol{F}_{\mathrm{CZF}}\} = &\underset{\{\boldsymbol{P},\boldsymbol{B},\boldsymbol{F}\}}{\operatorname{argmin}} \sum_{k=1}^K \varepsilon_k \\ \text{subject to: } &\boldsymbol{B}\boldsymbol{H}\boldsymbol{P} = \boldsymbol{\Pi}^{\mathrm{T}}(\boldsymbol{I}_K - \boldsymbol{F}), \\ &\mathrm{E}[\|\boldsymbol{P}\boldsymbol{v}\|_2^2] \le E_{\mathrm{tr}}, \\ &\varepsilon_1 = a_k\varepsilon_k\ \forall k \\ &\boldsymbol{F} \text{ lower triangular, zero maindiagonal.}\end{aligned} \tag{36}$$

For our purpose, the sorting order $\boldsymbol{\Pi}$ is not included in the optimization. The solution of (36) reads as

$$\begin{aligned}\boldsymbol{P}_{\mathrm{CZF}} &= \sum_{k=1}^K b_{i_k}^{-1}\left(\boldsymbol{\Pi}_k^{(\mathcal{O})}\boldsymbol{H}\right)^+\boldsymbol{e}_{i_k}\boldsymbol{e}_k^{\mathrm{T}}, \\ \boldsymbol{F}_{\mathrm{CZF}} &= \boldsymbol{I}_K - \boldsymbol{\Pi}\boldsymbol{B}_{\mathrm{CZF}}\boldsymbol{H}\boldsymbol{P}_{\mathrm{CZF}},\end{aligned} \tag{37}$$

where we introduced $\boldsymbol{\Pi}_k^{(\mathcal{O})} = \boldsymbol{\Pi}^{\mathrm{T}}\boldsymbol{S}_k^{\mathrm{T}}\boldsymbol{S}_k\boldsymbol{\Pi} \in \{0,1\}^{K\times K}$ with the sorting order $\mathcal{O} = (i_1,\ldots,i_K)$, $(\cdot)^+$ denotes the pseudo-inverse, and $\boldsymbol{S}_k = [\boldsymbol{I}_k, \boldsymbol{0}_{k\times(K-k)}] \in \{0,1\}^{k\times K}$ is a selection matrix. The single-user MSEs read as

$$\varepsilon_k = \frac{1}{a_k E_{\mathrm{tr}}}\sum_{m=1}^K \alpha_m\sigma_{v_m}^2\sigma_{\boldsymbol{\eta}_{i_m}}^2 a_{i_m}, \tag{38}$$

from which all $b_{\mathrm{CZF},k}$ an be computed via (35). For a shorter notation, we introduced the substitution

$$\alpha_k = \left[\left(\boldsymbol{S}_k\boldsymbol{\Pi}\boldsymbol{H}\boldsymbol{H}^{\mathrm{H}}\boldsymbol{\Pi}^{\mathrm{T}}\boldsymbol{S}_k^{\mathrm{T}}\right)^{-1}\right]_{k,k}. \tag{39}$$

Despite the sorting order and the modified expressions for the main diagonal elements of the inverse in (39), the two expressions in (38) and (8) are very similar. For the $K = 2$ users case, we obtain by eliminating the MSE quotient a_2

$$\frac{\sigma_{v_1}^2\alpha_1}{b_{i_1}^2} + \frac{\sigma_{v_2}^2\alpha_2}{b_{i_2}^2} = E_{\mathrm{tr}}, \tag{40}$$

which again can be transformed into the hyperbolic relationship similar to (12):

$$\varepsilon_2(\varepsilon_1) = \frac{\varepsilon_{\mathrm{inf},1}\varepsilon_{\mathrm{inf},2}}{\varepsilon_1 - \varepsilon_{\mathrm{inf},1}} + \varepsilon_{\mathrm{inf},2}, \tag{41}$$

with the infima now depending on the sorting order:

$$\varepsilon_{\mathrm{inf},k} = \frac{\sigma_{\nu_{i_k}}^2 \alpha_{i_k} \sigma_{\eta_k}^2}{E_{\mathrm{tr}}}. \tag{42}$$

For two users, two sorting orders are possible:

I) Sorting order 1: $\boldsymbol{\Pi} = \boldsymbol{I}_2$, $i_1 = 1$, $i_2 = 2$.

By replacing α_{i_k}, the infima read as

$$\begin{aligned} \varepsilon_{\mathrm{inf},1} &= \frac{\sigma_{\nu_1}^2 \sigma_{\eta_1}^2}{\|\boldsymbol{h}_1\|_2^2 E_{\mathrm{tr}}}, \\ \varepsilon_{\mathrm{inf},2} &= \frac{\sigma_{\nu_2}^2 \sigma_{\eta_2}^2}{\|\boldsymbol{h}_2\|_2^2 (1-|\varrho|^2) E_{\mathrm{tr}}}. \end{aligned} \tag{43}$$

Compared to Eq. (13), the SNR-decreasing penalty term $1/(1-|\varrho|^2)$ resulting from the interference suppression appears only once. This follows from the non-linear feedback, since for this sorting order, the constraint $\boldsymbol{h}_2^{\mathrm{T}} \boldsymbol{p}_1 = 0$ does not need to hold, cf. the constraint $\boldsymbol{BHP} = \boldsymbol{I}_2 - \boldsymbol{F}$ in (36).

II) Sorting order 2: $\boldsymbol{\Pi} = \boldsymbol{e}_1 \boldsymbol{e}_2^{\mathrm{T}} + \boldsymbol{e}_2 \boldsymbol{e}_1^{\mathrm{T}}$, $i_1 = 2$, $i_2 = 1$.

For this sorting kind, we obtain

$$\begin{aligned} \varepsilon_{\mathrm{inf},1} &= \frac{\sigma_{\nu_2}^2 \sigma_{\eta_1}^2}{\|\boldsymbol{h}_1\|_2^2 (1-|\varrho|^2) E_{\mathrm{tr}}}, \\ \varepsilon_{\mathrm{inf},2} &= \frac{\sigma_{\nu_1}^2 \sigma_{\eta_2}^2}{\|\boldsymbol{h}_2\|_2^2 E_{\mathrm{tr}}}. \end{aligned} \tag{44}$$

Here, the constraint $\boldsymbol{h}_1^{\mathrm{T}} \boldsymbol{p}_2 = 0$ required for the *linear* CZF filter can be dropped, since $\boldsymbol{BHP} = \boldsymbol{\Pi}^{\mathrm{T}} (\boldsymbol{I}_2 - \boldsymbol{F})$, and consequently, the penalty term $1/(1-|\varrho|^2)$ only affects the infimum $\varepsilon_{\mathrm{inf},1}$ of user 1.
Due to the modulo operation, a simple mapping from MSEs to data rates is not possible because the modulo operator leads to a non-Gaussian distribution of the noise realizations.

5. GRAPHICAL ILLUSTRATION

For the parameters $\|\boldsymbol{h}_1\|_2^2 = 3.2$, $\|\boldsymbol{h}_2\|_2^2 = 0.8$, and $|\varrho|^2 = 0.5$, the MSE borders from Subsection 3.1 of the linear CZF filter (star marker) and from Section 4 of the non-linear THP version are shown in Fig. 8. The transmit power E_{tr} is set to 5, moreover, for the symbol and noise variances, $\sigma_{s_1}^2 = \sigma_{s_2}^2 = 1$ and $\sigma_{\eta_1}^2 = \sigma_{\eta_2}^2 = 1$ hold, and the modulation alphabet is QPSK. In the linear case (star marker), the curve has a smaller abscissa offset $\varepsilon_{\mathrm{inf},1} = 0.125$ than an ordinate offset $\varepsilon_{\mathrm{inf},2} = 0.5$, since the instantaneous channel power $\|\boldsymbol{h}_1\|_2^2$ of user 1 is larger than the one of user 2. If Tomlinson-Harashima-precoding is applied, two sorting orders become possible. For order 1 from case I) in Section 4

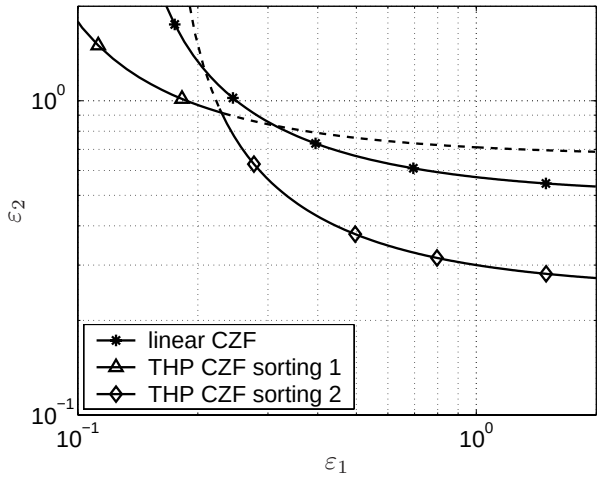

Figure 8. Border of MSE region for the linear CZF (star marker) and the non-linear CZF with THP and two sorting orders (triangle-up / rhomb marker), $E_{\mathrm{tr}} = 5$, QPSK.

(triangle up marker) the filter vector $\boldsymbol{p}_1$ may generate interference to user 2, since it is removed by the non-linear structure and the feedback filter $\boldsymbol{F}$. Hence, the infimum $\varepsilon_{\mathrm{inf},1}$ features the factor $(1-|\varrho|^2)\sigma_{s_1}^2/\sigma_{\nu_1}^2 = 0.5$ compared to the linear CZF. In contrast, the (weaker) second user has to suppress the interference via $\boldsymbol{p}_2$ *and* has to face the precoding loss $\sigma_{\nu_2}^2/\sigma_{s_2}^2 = 4/3$, so the hyperbola is very asymmetric. A more symmetric one is achieved by choosing sorting order II): The spatial filter $\boldsymbol{p}_1$ for the stronger user 1 has to suppress its interference caused at user 2, whereas user 2 is not affected by the term $1-|\varrho|^2$ (see Eq. 44).

The borders of the bit error probability regions feasible for the linear constrained zero-forcing filter are shown in Fig. 9 for $E_{\mathrm{tr}} = 5$ and the QPSK modulation alphabet. The unsymmetric behavior known from the MSE region translates itself into the fact that user 1 can achieve much smaller values of the uncoded BEP. From (19), we find $p_{\mathrm{inf},1} \approx 0.0023$ and $p_{\mathrm{inf},2} \approx 0.0786$.

Fig. 10 visualizes the borders of the *rate* regions for $E_{\mathrm{tr}} = 5$ (star marker) and $E_{\mathrm{tr}} = 1$ (circle marker). If $E_{\mathrm{tr}} = 5$, the (normalized) supremum $R_{\mathrm{sup},1}$ of the data rate R_2 of user 2 is approx. 3.17, and $R_{\mathrm{sup},2} \approx 1.58$, see (22). The *sum* rate corresponds to the radial distance of the curve with the triangle-down marker to the origin. The maximum sum rate is achieved for $R_{\Sigma-\max,1} = \log_2 13 - 1 \approx 2.7$ and $R_{\Sigma-\max,1} = \log_2 \frac{26}{8} - 1 \approx 0.7$, cf. (26). The difference $R_{\Sigma-\max,1} - R_{\Sigma-\max,2}$ achieving maximum sum rate follows from (27) and is identical to 2 in this case, whereas the sum $R_{\Sigma-\max,1} + R_{\Sigma-\max,2}$ corresponds to the length of the dash-dotted line.
When the transmit power is reduced to $E_{\mathrm{tr}} = 1$, the border of the rate region has the circle marker, and the sum rate is the radial coordinate of the curve with the cross marker.

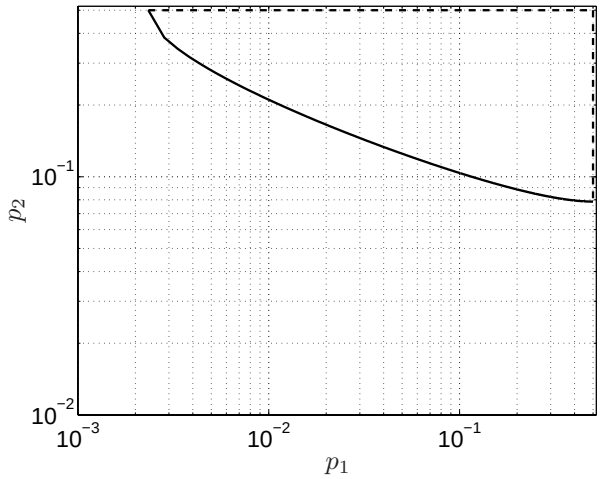

Figure 9. Border of the bit error probability (BEP) region of the linear CZF for $E_{\mathrm{tr}} = 5$, QPSK.

Because of the small value of E_{tr}, inequality (24) does not hold, and consequently, the maximum *sum* rate follows from asymptotically discarding user 2, see (28). The intersection between the border curve of the rate region and the piecewise affine curve with the square marker yields the rates $R_{\Sigma-\mathrm{sup},k}$.

6. CONCLUSION

We have presented a convenient description of the achievable MSE, SNR, BEP, and rate regions which are supported by the physical layer when the constrained zero-forcing filter is applied. Thus, the higher OSI layers are enabled to choose the operating point out of these sets in a straightforward manner according to the requested quality of service. Our approach can be applied to both linear and non-linear precoding schemes.

7. REFERENCES

[1] R. L. Choi and R. D. Murch, "Transmit MMSE pre-RAKE pre-processing with simplified receivers for the downlink of MISO TDD-CDMA systems," in *Global Telecommunications Conference (Globecom '02)*, November 2002, vol. 1, pp. 429–433.

[2] P. W. Baier, M. Meurer, T. Weber, and H. Tröger, "Joint Transmission (JT), an alternative rationale for the downlink of time division CDMA using multi-element transmit antennas," in *Proc. ISSSTA'00*, Parsippany, Sept. 2000, vol. 1, pp. 1–5.

[3] R. Fischer, *Precoding and Signal Shaping for Digital Transmission*, John Wiley & Sons, 2002.

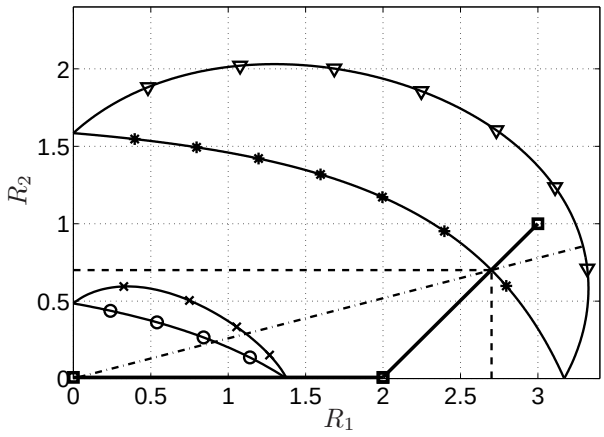

Figure 10. Border of rate region for $E_{\mathrm{tr}} = 5$ (star marker), and $E_{\mathrm{tr}} = 1$ (circle marker), respectively. The sum rates correspond to the curves with the triangle down and cross marker, respectively.

[4] M. Joham, W. Utschick, and J. A. Nossek, "Linear Transmit Processing in MIMO Communications Systems," *Accepted for publication in IEEE Transactions on Signal Processing*, 2004.

[5] S. Shi and M. Schubert, "MMSE Transmit Optimization for Multi-User Multi-Antenna Systems," in *Proc. ICASSP 2005*, March 2005.

[6] R. Irmer, W. Rave, and G. Fettweis, "Minimum BER transmission for TDD-CDMA in frequency-selective channels," in *Proc. IEEE PIMRC*, September 2003, pp. 1260–1264.

[7] R. Hunger, M. Joham, and W. Utschick, "Extension of Linear and Nonlinear Transmit Filters for Decentralized Receivers," *Accepted for presentation at European Wireless 2005*, April 2005.

[8] D. Reynolds, A. Høst Madsen, and X. Wang, "Adaptive Transmitter Precoding for Time Division Duplex CMDA in Fading Multipath Channels: Strategy and Analysis," *EURASIP Journal of Applied Signal Processing*, , no. 12, pp. 1325–1334, December 2002.

[9] A. Scaglione, P. Stoica, G. Giannakis, S. Barbarossa, and H. Sampath, "Optimal Designs for Space-Time Linear Precoders and Decoders," *IEEE Transactions on Signal Processing*, vol. 50, no. 5, pp. 1051–1064, May 2002.

[10] D. P. Palomar, J. M. Cioffi, M.A. Lagunas, and A. Pascual, "Convex Optimization Theory Applied to Joint Beamforming Design in Multicarrier MIMO

Systems," in *Proc. IEEE 2003 International Conference on Communications (ICC 2003)*, May 2003, vol. 4, pp. 2974–2978.

[11] J. A. Nossek, M. Joham, and W. Utschick, "Transmit Processing in MIMO Wireless Systems," in *6th CAS Symposium on Emerging Technologies*, May 2004, vol. I, pp. I–18–I–23.

[12] R. Hunger, F. Dietrich, M. Joham, and W. Utschick, "Robust Transmit Zero-Forcing Filters," in *Proc. ITG Workshop on Smart Antennas*, March 2004.

[13] F. Rey, M. Lamarca, and G. Vázquez, "Optimal Power Allocation with Partial Channel Knowledge for MIMO Multicarrier Systems," in *Proc. VTC Fall*, September 2002, vol. 4, pp. 2121–2125.

[14] R. Fischer, C. Windpassinger, A. Lampe, and J. Huber, "MIMO Precoding for Decentralized Receivers," in *Proceedings of International Symposium on Information Theory (ISIT '02)*, 2002, p. 496.

[15] R. Fischer, C. Windpassinger, A. Lampe, and J. Huber, "Space-Time Transmission using Tomlinson-Harashima Precoding," in *Proceedings of 4. ITG Conference on Source and Channel Coding (SCC '02)*, January 2002, pp. 139–147.

[16] J. Liu and A. Duel-Hallen, "Tomlinson-Harashima Transmitter Precoding for Synchronous Multiuser Communications," in *Proc. 37th Annual Conference on Information Science and Systems (CISS '03)*, March 2003.

[17] M. Joham, J. Brehmer, and W. Utschick, "MMSE Approaches to Multiuser Spatio-Temporal Tomlinson-Harashima Precoding," in *Proc. ITG SCC'04*, January 2004, pp. 387–394.